Polymers **2012**, *4*, 1613-1626; doi:10.3390/polym4031613

OPEN ACCESS

polymers

ISSN 2073-4360

www.mdpi.com/journal/polymers

Article

Dye-sensitized Solar Cells with New One-Dimensional Halide-Bridged Cu(I)–Ni(II) Heterometal Coordination Polymers Containing Hexamethylene Dithiocarbamate Ligand

Takashi Okubo [1,*], Naoya Tanaka [1], Haruho Anma [1], Kyung Ho Kim [2], Masahiko Maekawa [1] and Takayoshi Kuroda-Sowa [1]

[1] School of Science and Engineering, Kinki University, 3-4-1 Kowakae, Higashi-Osaka-shi, Osaka 577-8502, Japan; E-Mails: nekonikobam@yahoo.co.jp (N.T.); nma_chem_sci_kindai@yahoo.co.jp (H.A.); maekawa@rist.kindai.ac.jp (M.M.); kuroda@chem.kindai.ac.jp (T.K.S.)

[2] Department of Materials Science and Engineering, Kitami Institute of Technology, 165 Koen-cho, Kitami, Hokkaido 090-8507, Japan; E-Mail: khkim@mail.kitami–it.ac.jp

***** Author to whom correspondence should be addressed; E-Mail: okubo_t@chem.kindai.ac.jp; Tel.: +81-6-6730-5880-4117; Fax: +81-6-6723-2721.

Received: 2 July 2012; in revised form: 5 September 2012 / Accepted: 10 September 2012 / Published: 20 September 2012

Abstract: One-dimensional (1D) halide-bridged Cu(I)–Ni(II) heterometal coordination polymers containing a hexamethylene dithiocarbamate (Hm-dtc) ligand have been synthesized and crystallographically characterized. The highest occupied molecular orbital (HOMO) and lowest unoccupied molecular orbital (LUMO) levels of the coordination polymers were estimated using UV-Vis-NIR and photoelectron spectroscopies, and it was revealed that these coordination polymers have appropriate HOMO levels for use as dye sensitizers. Direct-current electrical conductivity measurements and impedance measurements indicated that these 1D Cu(I)–Ni(II) heterometal coordination polymers were insulators ($\sigma_{300K} < 10^{-12}$ S cm^{-1}). In addition, the coordination polymers were used as sensitizing materials in dye-sensitized solar cells (DSSCs). DSSCs with 1D Cu(I)–Ni(II) heterometal coordination polymers showed lower performances than those with 1D halide-bridged Cu(I)–Cu(II) mixed-valence coordination polymers.

Keywords: coordination polymer; crystal structure; electric-conductivity; dye-sensitized solar cell

1. Introduction

Crystal engineering of coordination polymers is one of the most attractive subjects in the field of materials science because of the polymers' versatile chemical and physical properties such as magnetic [1–3] and conductive [4–14], dielectric [15–17], gas-absorbing [18–20], and catalytic properties [21–24]. One of the most attractive areas in this field is the synthesis of conductive coordination polymers, in terms of both fundamental topics such as d-π systems [25] and applications to novel optoelectronic devices such as electroluminescent (EL) devices [26], field-effect transistors (FETs), and solar cells [27]. However, the applications of coordination polymers in semiconducting materials for solar cells are less developed than those of conventional mononuclear complexes such as copper phthalocyanines [28,29] and ruthenium complexes [30,31], even although coordination polymers have regular networks for the conductive pathways of photogenerated electrons.

Dithiocarbamate derivatives are promising bridging ligands for formation of coordination polymers with the potential to be semiconducting materials [12–14]. The overlaps of the d-orbitals and highest occupied molecular orbitals (HOMOs) and/or lowest unoccupied molecular orbitals (LUMOs) of the ligands in Cu(II)–dithiocarbamate coordination polymers result in the formation of narrow conduction and/or valence bands, inducing strong magnetic interactions and conducting properties. Recently, we demonstrated that one-dimensional (1D) mixed-valence Cu(I)–Cu(II) coordination polymers containing a dithiocarbamate ligand and bromide or iodide anions, $[Cu^{I}_{2}Cu^{II}X_{2}(Hm\text{-}dtc)_{2}(CH_{3}CN)_{2}]_{n}$ [Hm-dtc = hexamethylene dithiocarbamate; X = Br^{-} (**2a**), I^{-} (**2b**)], exhibited semiconducting properties at relatively small activation energies [σ_{340K} = 1.07 × 10^{-7} S cm^{-1}, E_a = 0.56 eV, (**2a**); σ_{340K} = 2.46 × 10^{-7} S cm^{-1}, E_a = 0.48 eV (**2b**)] [12], and these polymers could be used as sensitizing materials for dye-sensitized solar cells (DSSCs) [27]. In addition, a three-dimensional (3D) mixed-valence Cu(I)–Cu(II) coordination polymer, $\{[Cu^{I}_{4}Cu^{II}_{2}Br_{4}(Pyr\text{-}dtc)_{4}]\cdot CHCl_{3}\}_{n}$ (Pyr-dtc = pyrrolidine dithiocarbamate; (**3**), showed high conductivity (σ_{300K} = 5.2 × 10^{-7} S cm^{-1}, E_a = 0.29 eV); this was investigated using an impedance spectroscopy technique and flash-photolysis time-resolved microwave conductivity measurements [13]. However, the DSSC with this coordination polymer showed lower power conversion efficiency (PCE, η) than those with the 1D coordination polymers **2a** and **2b**, because the LUMO level of **3** is lower than that of the conduction band of a TiO_2 semiconductor (−4.0 eV) [32], as shown in this paper.

Now it is becoming an important issue to search the coordination polymers suitable for dye materials of DSSCs. Studies on the solar cells with the coordination polymers, however, are less developed than those with the organic semiconductors, and to the best of our knowledge, there has been no example of the application of the coordination polymers to solar cell devices, other than our research mentioned above, although the coordination polymers have many advantages as new dye materials in terms of the diversity, designability and possibility of new functional materials. In addition, there is insufficient knowledge to design new semiconducting materials. Thus, we attempted to investigate the DSSCs with new 1D halide-bridged Cu(I)–Ni(II) heterometal coordination polymers containing Hm-dtc; these have crystal structures isomorphous to those of the 1D mixed-valence Cu(I)–Cu(II) coordination polymers **2a** and **2b**, which were the first examples of the dithiocarbamate coordination polymers including Ni(II) ion, in order to accumulate scientific knowledge for developing new functional materials based on the coordination polymers. In this paper, we describe the synthesis,

X-ray crystal structures, conducting and dielectric properties of new 1D halide-bridged Cu(I)–Ni(II) heterometal coordination polymers, $[Cu^{I}_{2}Ni^{II}X_2(Hm\text{-}dtc)_2(CH_3CN)_2]_n$ [X = Br^- (**1a**), I^- (**1b**)] and we also compare the photovoltaic properties of DSSCs containing **1a**, **1b**, **2a**, **2b** and **3** with those of DSSCs containing semiconducting Cu(I)–Cu(II) mixed-valence coordination polymers as sensitizing dyes.

2. Experimental Section

2.1. Materials

A mononuclear metal complex, $Ni(Hm\text{-}dtc)_2$, was prepared using a procedure similar to that previously reported [33,34]. The reagents were purchased from Tokyo Kasei Kogyo Co., Ltd. (Tokyo, Japan) and Aldrich Chemical Co., Inc. (St Louis, MO, USA). All the chemicals were used without further purification.

*2.2. Synthesis of $[Cu^{I}_{2}Ni^{II}Br_2(Hm\text{-}dtc)_2(CH_3CN)_2]_n$ (**1a**)*

An acetonitrile solution (10 mL) of $CuBr{\cdot}S(CH_3)_2$ (0.041 g, 0.2 mmol) was diluted with 10 mL of acetone, and this solution was added to 20 mL of a $CHCl_3$ solution of $Ni(Hm\text{-}dtc)_2$ (0.041 g, 0.10 mmol). The reaction mixture was stirred for 5 min and then filtered. Crystals of complex **1a** suitable for X-ray analysis were obtained from the filtrate in several days. Anal. Calcd for $[Cu^{I}_{2}Ni^{II}Br_2(Hm\text{-}dtc)_2(CH_3CN)_2]_n$ ($C_{18}H_{30}Br_2Cu_2N_4NiS_4$): C, 27.85; H, 3.90; N, 7.22. Found: C, 27.64; H, 3.81; N, 7.18.

*2.3. Synthesis of $[Cu^{I}_{2}Ni^{II}I_2(Hm\text{-}dtc)_2(CH_3CN)_2]_n$ (**1b**)*

An acetonitrile solution (10 mL) of CuI (0.038 g, 0.2 mmol) was diluted with 10 mL of acetone, and this solution was added to 20 mL of a $CHCl_3$ solution of $Ni(Hm\text{-}dtc)_2$ (0.041 g, 0.10 mmol). The reaction mixture was stirred for 5 min and then filtered. Crystals of complex **1b** suitable for X-ray analysis were obtained from the filtrate in several days. Anal. Calcd for $[Cu^{I}_{2}Ni^{II}I_2(Hm\text{-}dtc)_2(CH_3CN)_2]_n$ ($C_{18}H_{30}Cu_2I_2N_4NiS_4$): C, 24.84; H, 3.47; N, 6.44. Found: C, 24.67; H, 3.43; N, 6.41.

2.4. Crystal Structure Determination

Data collections of the crystals for complex **1a** and **1b** were performed on a Rigaku RAXIS RAPID imaging plate area detector with graphite-monochromated Mo-Kα (λ = 0.71073 Å) radiation. The crystal structures were solved by direct methods (SHELX97 [35] for **1a** and SIR2008 [36] for **1b**) and expanded using the Fourier techniques. The non-hydrogen atoms were refined anisotropically. Hydrogen atoms were refined using the riding model. The final cycles of full-matrix least-squares refinement [37] on F^2 for **1a** and **1b** were based on 2966 and 3060 observed reflections and 142 and 142 variable parameters, respectively. All calculations were performed using the CrystalStructure [38] crystallographic software package except for refinement, which was performed using SHELXL-97 [35].

2.5. Fabrication of DSSCs

The coordination polymers (0.3 mol), $[Cu^{I}_2Ni^{II}X_2(Hm\text{-}dtc)_2(CH_3CN)_2]_n$ [X = Br^- (**1a**), I^- (**1b**)], $[Cu^{I}_2Cu^{II}X_2(Hm\text{-}dtc)_2(CH_3CN)_2]_n$ [X = Br^- (**2a**), I^- (**2b**)] and $\{[Cu^{I}_4Cu^{II}_2Br_4(Pyr\text{-}dtc)_4]\cdot CHCl_3\}_n$ (**3**) were mixed with TiO_2 paste (0.1 mL) for the electrode, where the TiO_2 paste for low-temperature sintering (PECC-K01) was purchased from Peccell Technologies Co. (Kanagawa, Japan) and the mixtures of the TiO_2 paste and the coordination polymers were grinded in a mortar for 10 min, and painted on an indium tin oxide (ITO, sheet resistance 10 Ω/sq) glass substrate with spacers of Kapton tape (thickness 50 μm). It was annealed at 50 °C for 0.5 h. For the counter-electrode, a solution of poly(3,4-ethylenedioxythiophene)-tetramethacrylate (PEDOT-TMA) was mixed with ethanol at a volume ratio of 5:1. The mixed solution was spin-coated (2000 rpm for 10 s) on ITO glass and annealed at 50 °C for 10 min. The two prepared electrodes were assembled to fabricate a sandwich-type cell with a 50-μm spacer, and the electrolyte, which was a solution of lithium iodide (LiI, 0.5 M) and iodine (I_2, 0.05 M) in polyethylene glycol, was injected between the electrodes. The performance of the solar cell was measured under irradiation with an AM 1.5 G (100 mW/cm^2) solar simulator (Bunkoukeiki Co., KP-3201). The cell device area was 0.30 cm^2.

2.6. Physical Measurements

UV-Vis-NIR spectra were monitored on a U-4100 UV/VIS/NIR Spectrophotometer (HITACHI). The photoemission yield spectra were measured by Surface Analyzer AC-2 (RIKEN KEIKI Co.). The DC conductivities were investigated with an Ultra High Resistance Meter R8340 (ADVANTEST) on a pellet of the powder sample sandwiched by 13 mm diameter brass electrodes. The impedance and dielectric measurements were carried out on a pellet of the powder sample sandwiched by 13 mm diameter brass electrodes with a 6440B (Wayne Kerr Electronics) Series Precision Component Analyzer in a frequency range 100 to 3 MHz.

3. Results and Discussion

3.1. Description of Crystal Structures

Single-crystal X-ray analysis of complex **1a** reveals the formation of a coordination polymer, $[Cu_2NiBr_2(Hm\text{-}dtc)_2(CH_3CN)_2]_n$, with a 1D infinite chain structure [39], as shown in Figure 1a. This complex consists of mononuclear copper units, $Ni(Hm\text{-}dtc)_2$, and dinuclear copper units, $Cu_2Br_2(CH_3CN)_2$, with bromide ions and acetonitrile molecules to construct the 1D infinite chain. The nickel ion of the mononuclear unit, Ni1, has a square-planar coordination geometry containing four sulfur atoms of two dithiocarbamate ligands, which form four-membered chelate rings. Each copper ion in the dinuclear unit, Cu1, has a distorted tetrahedral coordination geometry with two bridging bromide anions, one nitrogen atom of acetonitrile, and one sulfur atom of the mononuclear unit. In the mononuclear $Ni(Hm\text{-}dtc)_2$ unit of the coordination polymer **1a**, the average Ni1–S distance (2.2212(7) Å) is slightly longer than those of the typical average Ni(II)–S distances in Ni(II)–dithiocarbamate complexes such as $Ni^{II}(EtOH_2dtc)_2$ (2.201 Å) [40], $Ni^{II}(Pip\text{-}dtc)_2$ (2.202 Å) [41], $Ni^{II}(echdtc)_2$ (2.2056 Å) [42] and $Ni^{II}\{S_2CN(CH_2CH_2OMe)_2\}_2$ (2.2038 Å) [43], and is shorter than

those in Cu(II)–dithiocarbamate complexes [33] such as $Cu^{II}(Me_2dtc)_2$ (2.3105 Å), $Cu^{II}(Et_2dtc)_2$ (2.3117 Å), $Cu^{II}(n\text{-}Pr_2dtc)_2$ (2.3183 Å) and $Cu^{II}(i\text{-}Pr_2dtc)_2$ (2.2886 Å). The structural data for the Ni1–S distances therefore indicate that the Ni1 ion is divalent. The Cu1 ion in the dinuclear unit has a distorted-tetrahedral coordination geometry typical of monovalent copper ions. The Cu1–Br1 and Cu1–Br1* distances are 2.4638(4) Å and 2.5519(5) Å, respectively. In order to confirm the oxidation state of the Cu1 ion, we performed bond valence sum (BVS) calculations [44]. The estimated BVS value for the Cu1 ion was 1.19, indicating the monovalent oxidation state. On the basis of its charge neutrality, it is concluded that the chemical formula of **1a** is $[Cu^{I}_2Ni^{II}Br_2(Hm\text{-}dtc)_2(CH_3CN)_2]_n$; the square-planar Ni1 of the mononuclear unit $Ni(Hm\text{-}dtc)_2$ is divalent and the tetrahedral Cu1 in the dinuclear unit is monovalent. Figure 1c shows the packing diagram of the 1D chains for complex **1a**, viewed parallel to the *a*-axis. The nearest-neighbor S•••S, S•••Br, and Cu•••Cu separations between the 1D chains were 3.8910(6) Å, 6.9921(3) Å, and 8.1909(6) Å, respectively. These separations were larger than those of the sums of the van der Waals radii of the sulfur, bromide, and copper atoms.

Figure 1. Infinite chain structures of 1D Cu(I)–Ni(II) heterometal coordination polymers of **1a** (**a**) and **1b** (**b**); packing diagrams of **1a** (**c**) and **1b** (**d**) viewed parallel to the *a*-axis: Cu, red-brown; Br, orange; I, purple; S, yellow; C, white; and N, blue. Hydrogen atoms are omitted for clarity.

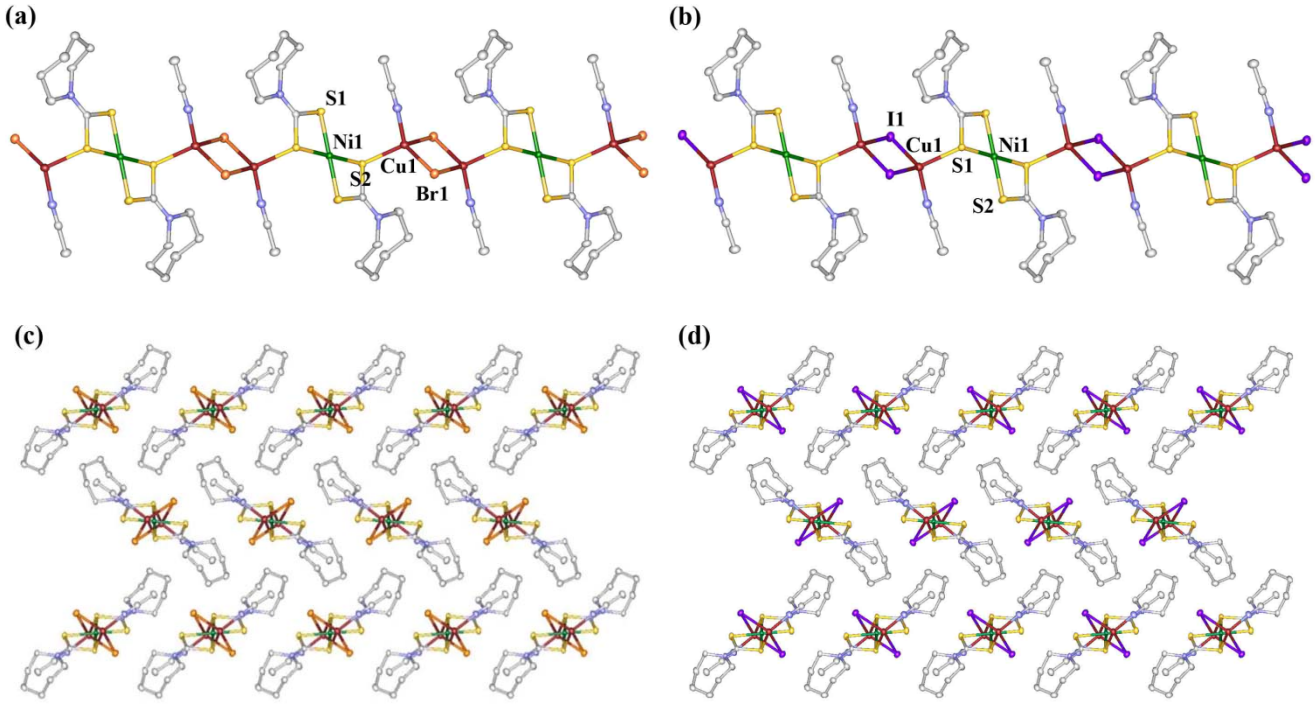

$[Cu^{I}_2Ni^{II}I_2(Hm\text{-}dtc)_2(CH_3CN)_2]_n$ (**1b**), which contains iodide ions, is isostructural (Figure 1b) [45] with complex **1a**. The average Ni1–S distance (2.2113(8) Å) in the mononuclear unit is similar to that of complex **1a**, and the estimated BVS value for the Cu1 ion with tetrahedral coordination geometry is 1.19. The packing diagram of the 1D chains for complex **1b** is shown in Figure 1d. The nearest-neighbor S•••S, S•••Br, and Cu•••Cu separations between the 1D chains were 4.0004(3) Å, 6.9452(8) Å, and 8.2724(8) Å, respectively.

*3.2. Determination of HOMO and LUMO Levels of **1a** and **1b***

Figure 2a shows the absorption spectra obtained via diffuse reflectance spectroscopy of the mononuclear complex Ni(Hm-dtc)$_2$ (black) [46] (Figure S1 in the Supporting Information), and coordination polymers **1a** (red) and **1b** (blue), doped in MgO; the measurements were carried out with pellet samples made by mixing each metal complex (0.01 mmol) with MgO powder (80 mg); the absorbances were plotted as the Kubelka–Munk function [47]:

$$\text{Kubelka} - \text{Munk} = f(R) = (1 - R^2)/2R \quad (1)$$

where R is the absolute reflectance of the samples. The 1D coordination polymers exhibit two absorption bands in the visible region. The larger absorption bands at around 380 nm for Ni(Hm-dtc)$_2$, **1a**, and **1b** could be attributed to charge transfer. The small absorption bands at around 640 nm for Ni(Hm-dtc)$_2$, **1a**, and **1b** may arise from d–d transitions of the nickel(II) ion. The HOMO–LUMO gaps (band gaps) of the Ni(Hm-dtc)$_2$ coordination polymers **1a** and **1b** were estimated from the absorption edges (Figure 3b) to be 1.58 eV, 1.34 eV, and 1.57 eV, respectively. The HOMO–LUMO gaps of the coordination polymer **1a** are smaller than those of **1b** and those of other 1D coordination polymers with dithiocarbamate ligands, such as 1.48 eV for **2a** and 1.48 eV for **2b**, and larger than that of the 3D coordination polymer **3** (1.01 eV). In order to compare the absorption intensity, the transmission spectra with the KBr powder pressed pellets including the coordination polymers **1a**, **1b**, **2a** and **2b** (0.5 μmol in 50 mg KBr) were measured and shown in Figure S3, which indicates the decreasing of the transition probability of the d-d transitions around 600 nm for the Cu(I)–Ni(II) heterometal coordination polymers **1a** and **1b** as against the Cu(I)–Cu(II) mixed-valence coordination polymers **2a** and **2b.**

Figure 2. (**a**) Diffuse-reflection UV-Vis-NIR absorption spectra of mononuclear complex Ni(Hm-dtc)$_2$ (black), and coordination polymers **1a** (red), and **1b** (blue) (0.01 mmol), doped in MgO powder (80 mg), obtained via Kubelka–Munk analysis of reflectance spectra; (**b**) Plots of modified Kubelka–Munk function versus energy of exciting light.

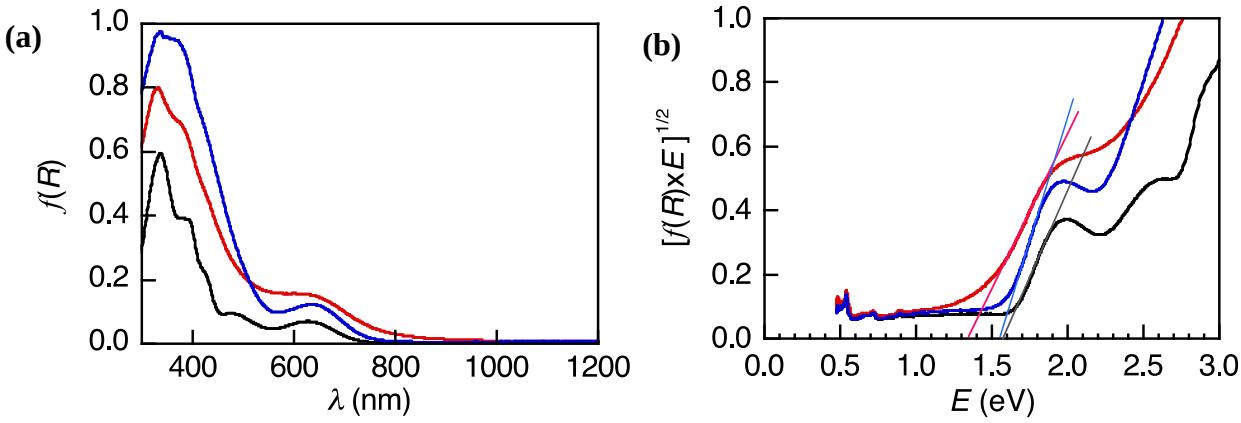

The photoemission yield curves of the coordination polymers **1a** and **1b** are shown in Figure 3. The HOMO energy levels of complexes **1a**, **1b**, and **3** (Figure S2) are −5.24, −5.23, and −5.28 eV, respectively. These values are sufficiently low for the complexes to accept electrons from the redox electrolyte (−4.8 eV). From the HOMO values, the LUMO energy levels obtained from the band edges

of the absorption spectra are determined to be −3.90 eV for **1a**, −3.66 for **1b**, and −4.27 eV for **3**. These indicate that the energy level of the LUMO for the 3D coordination polymer **3** is lower than that of the conduction band (E_{CB}) of the TiO_2 semiconductor (−4.0 eV); in contrast, the energy levels of the LUMO for the 1D Cu(I)–Ni(II) heterometal coordination polymers **1a** and **1b** are well matched with the E_{CB} of the TiO_2 semiconductor, enabling electron injection from the dyes **1a** and **1b**.

Figure 3. Photoemission yield curves of the coordination polymers **1a** (red) and **1b** (blue) under atmospheric conditions.

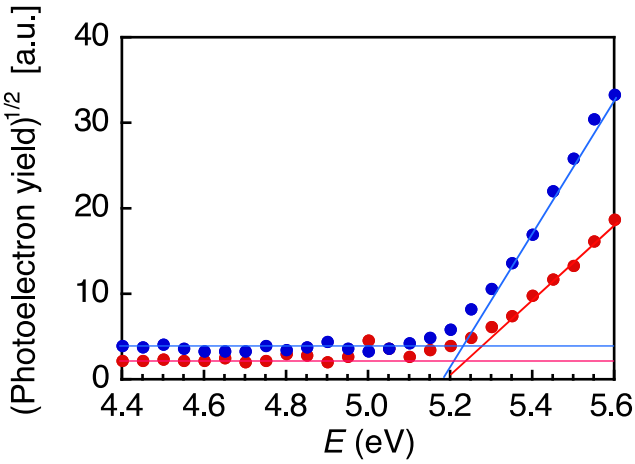

*3.3. Electroconducting and Dielectric Properties of **1a** and **1b***

Most of the Cu(I)–Cu(II) mixed-valence coordination polymers with dithiocarbamate ligands show semiconducting properties because the overlaps of the d-orbitals and HOMOs and/or LUMOs of the ligands in the Cu(II)–dithiocarbamate coordination polymers cause the formation of narrow conduction and/or valence bands, inducing strong magnetic interactions and conducting properties. It is predicted that Cu(I)–Ni(II) heterometal coordination polymers containing Ni(II)–dithiocarbamate units will show lower conductivities than those of Cu(I)–Cu(II) mixed-valence coordination polymers with dithiocarbamate ligands since the overlaps of the d-orbitals and the HOMOs and/or LUMOs of the dithiocarbamate ligands in the Cu(I)–Ni(II) coordination polymers are smaller than those in the Cu(II)–dithiocarbamate coordination polymers because of the higher d-levels of the nickel(II) ions than those of copper(II) ions. The direct-current (DC) electrical resistivities of powder-pressed pellet samples of the coordination polymers **1a** and **1b**, sandwiched by brass electrodes (diameter 13 mm), were measured in the temperature range 250–400 K. The thicknesses of the pellet samples of the coordination polymers **1a** and **1b** were 0.239 mm and 0.164 mm, respectively, and the applied DC voltage was 100 V. The variations in the DC conductivities of **1a** (red) and **1b** (blue) at different temperatures are shown in Figure 4. The conductivities of the Cu(I)–Ni(II) coordination polymers **1a** and **1b** are smaller than those of the Cu(I)–Cu(II) mixed-valence coordination polymers **2a**, **2b**, and **3** by several orders of magnitude, and do not show the temperature dependences of thermally activated semiconductors below 350 K, that is, these 1D Cu(I)–Ni(II) heterometal coordination polymers were insulators ($\sigma_{300K} < 10^{-12}$ S cm^{-1}) below 350 K, and the observed DC conductivities below 350 K may be not as the bulk samples for the coordination polymers but as the leak current of the samples. The conducting properties of the Cu(I)–Ni(II) coordination polymers **1a** and **1b** were also investigated

using complex impedance spectroscopy—a powerful technique for studying the carrier transport and dielectric properties of bulk samples and electric devices. The impedance measurements were carried out using the same powder-pressed pellet sample. Most of the semiconducting samples show semicircular arcs in the Cole–Cole plots of the impedance and the electric modulus, but the Cole–Cole plots of the impedance and electric modulus for **1a** and **1b** do not show semicircular arcs because of their quite low conductivities. Figure 5a,b show the temperature and frequency dependencies of the dielectric properties converted from the impedance data. Both samples showed temperature and frequency independent dielectric properties below 350 K, which indicated the insulation properties of the Cu(I)–Ni(II) heterometal coordination polymers.

Figure 4. Temperature dependency of the direct-current (DC) conductivities of the coordination polymers **1a** (red) and **1b** (blue).

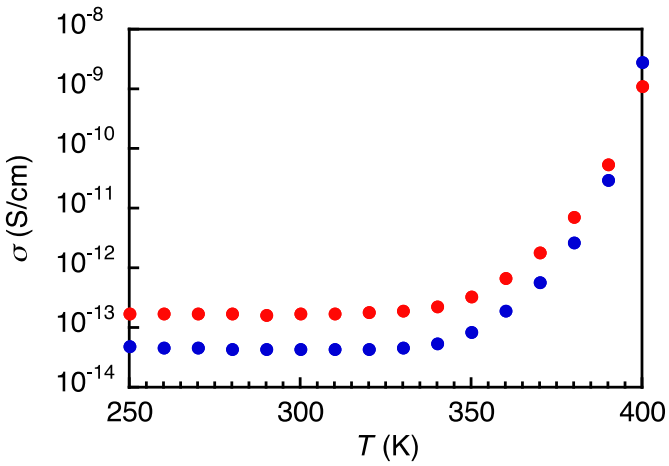

Figure 5. Dielectric properties of the coordination polymers **1a** (**a**) and **1b** (**b**) estimated from the impedance analysis.

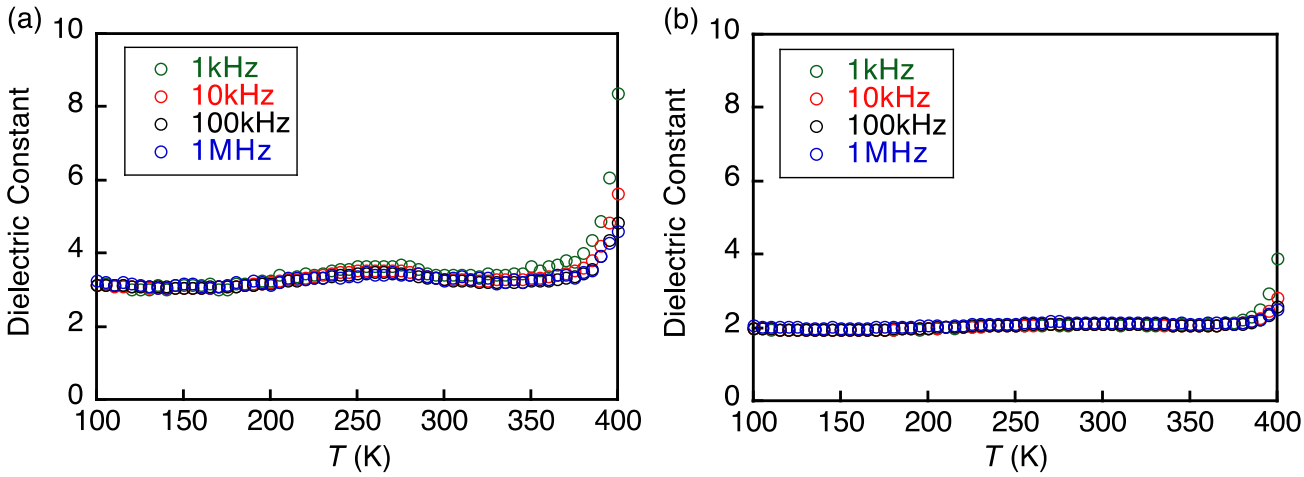

*3.4. Photovoltaic Performance of DSSCs with Coordination Polymers **1a**, **1b**, **2a**, **2b** and **3***

Research on solar cells containing coordination polymers is less developed than that on mononuclear metal complexes such as N3 dye ([Ru(4,4'-$(COOH)_2$-byy)$_2$$(NCS)_2$]) [30] and black dye ([Ru(4,4',4"-$(COOH)_3$-terpy)$(NCS)_3$]) [48], because the process of forming thin films of coordination

polymers is still undeveloped. This is because coordination polymers are generally insoluble in organic solvents and retain their infinite structures, and they do not have functional groups such as carboxyl groups to connect with the TiO_2 surface of the photoelectrode. To the best of our knowledge, there has been no example of the application of coordination polymers to solar cell devices, other than our research. In our research, the photoelectrodes of DSSCs were fabricated using TiO_2 paste for low-temperature sintering (PECC-K01, Peccell Technologies Co., Kanagawa, Japan), directly mixed with **1a**, **1b**, **2a**, **2b** or **3**. The mixtures were prepared by mixing the TiO_2 paste and the coordination polymer using an agate mortar. Figure 6 shows the photocurrent density–voltage (*J–V*) curves of the DSSCs with the 1D Cu(I)–Ni(II) heterometal coordination polymers $[Cu^{I}_2Ni^{II}X_2(Hm\text{-}dtc)_2(CH_3CN)_2]_n$ [X = Br^- (**1a**), I^- (**1b**)], the 1D Cu(I)–Cu(II) mixed-valence coordination polymers $[Cu^{I}_2Cu^{II}X_2(Hm\text{-}dtc)_2(CH_3CN)_2]_n$ [X = Br^- (**2a**), I^- (**2b**)], and the 3D Cu(I)–Cu(II) mixed-valence coordination polymer $\{[Cu^{I}_4Cu^{II}_2Br_4(Pyr\text{-}dtc)_4]\cdot CHCl_3\}_n$ (**3**). The details of the short-circuit current densities (J_{SC}), open-circuit voltages (V_{OC}), fill factors (FF), and PCEs (η) of cells with different coordination polymer dye materials are summarized in Table 1.

Figure 6. Photocurrent density–voltage (*J–V*) curves for dye-sensitized solar cells (DSSCs) with the coordination polymers **1a**, **1b**, **2a**, **2b** and **3**.

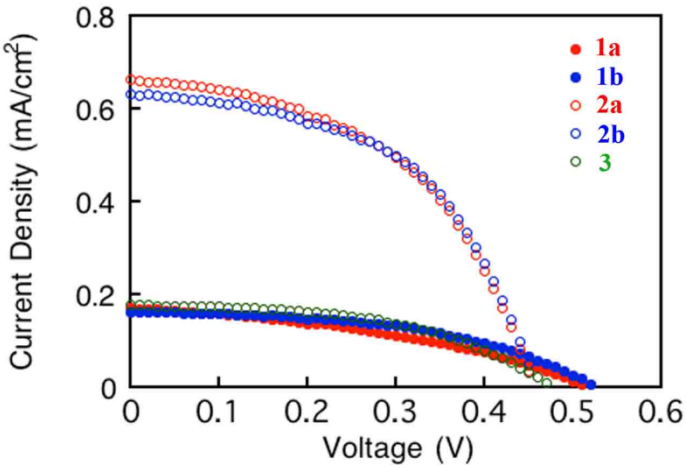

Table 1. Short-circuit current densities (J_{SC}), open-circuit voltages (V_{OC}), fill factors (FF), and power conversion efficiencies (PCE) for DSSCs with coordination polymers containing dithiocarbamate ligands.

Complex	J_{SC} (mA/cm)	V_{OC} (V)	FF	PCE (%)
1a	0.171	0.519	0.387	0.034
1b	0.163	0.527	0.489	0.041
2a	0.663	0.457	0.492	0.149
2b	0.633	0.460	0.519	0.151
3	0.177	0.478	0.492	0.041

The coordination polymers showing the highest performances in the DSSCs are the 1D Cu(I)–Cu(II) mixed-valence coordination polymers **2a** and **2b**, which have appropriate HOMO (−5.20 eV for **2a** and −5.10 eV for **2b**) and LUMO (−3.72 eV for **2a** and −3.62 eV for **2b**) levels as dye sensitizers, that is, the LUMO levels are higher than that of the conduction-band (E_{CB}) of the TiO_2 semiconductor

(−4.0 eV) and the HOMO levels are lower than that of the redox electrolyte (−4.8 eV). These coordination polymers also exhibit semiconducting properties (σ_{340K} = 1.07 × 10^{-7} S cm^{-1} for **2a** and σ_{340K} = 2.46 × 10^{-7} S cm^{-1} for **2b**) with small activation energies [E_a = 0.562 eV (**2a**) and E_a = 0.479 eV (**2b**)]. In contrast, the J_{SC} values for the DSSCs with the 1D Cu(I)–Ni(II) heterometal coordination polymers **1a** and **1b** are less than 1/3 of the J_{SC} values for **1a** and **1b**, although they also have appropriate HOMO (−5.24 eV for **2a** and −5.23 eV for **2b**) and LUMO (−3.90 eV for **1a** and −3.66 for **1b**) levels, as dye sensitizers. This might be the result of low absorptions in the visible region and the low conductivities of the 1D Cu(I)–Ni(II) heterometal coordination polymers **1a** and **1b**. The DSSC with the 3D Cu(I)–Cu(II) mixed-valence coordination polymer **3** shows lower efficiency than those with the 1D Cu(I)–Cu(II) mixed-valence coordination polymers **2a** and **2b**, and an efficiency similar to those of the 1D Cu(I)–Ni(II) heterometal coordination polymers **1a** and **1b**, despite the high conductivity of **3** as a semiconductor (σ_{300K} = 5.2 × 10^{-7} S cm^{-1}, E_a = 0.29 eV) and large absorption in the visible region [13]; this must be because the LUMO levels of **3** (−4.27 eV) are lower than that of the E_{CB} of TiO_2. The V_{OC} values for the DSSCs with the 1D Cu(I)–Ni(II) heterometal coordination polymers **1a** and **1b** are higher than those of the Cu(I)–Cu(II) mixed-valence coordination polymers **2a**, **2b**, and **3**. This difference may be attributed to the more strongly positive shift of the E_{CB} of TiO_2 in the case of the Cu(I)–Cu(II) mixed-valence coordination polymers **2a**, **2b**, and **3** [49].

4. Conclusions

We synthesized novel halide-bridged Cu(I)–Ni(II) heterometal coordination polymers with 1D infinite structures, which have appropriate HOMO and LUMO levels, as DSSC dye sensitizers. We fabricated DSSCs with the 1D Cu(I)–Ni(II) heterometal coordination polymers, and compared the photovoltaic properties of these DSSCs with those of DSSCs containing semiconducting Cu(I)–Cu(II) mixed-valence coordination polymers as sensitizing dyes.

Acknowledgments

This work was partly supported by PRESTO (JST) and a Grant-in-Aid for Science Research from the Ministry of Education, Culture, Sports, Science and Technology of Japan. And a part of this work was also conducted in Kyoto-Advanced Nanotechnology Network, supported by "Nanotechnology Network" of the Ministry of Education, Culture, Sports, Science and Technology (MEXT), Japan.

References and Notes

1. Kahn, O. *Molecular Magnetism*; VCH: New York, NY, USA, 1993.
2. Ferlay, S.; Mallah, T.; Ouahes, R.; Veillet, P.; Verdaguer, M. A room-temperature organometallic magnet based on Prussian blue. *Nature* **1995**, *378*, 701–703.
3. Sato, O.; Iyoda, T.; Fujishima, A.; Hashimoto, K. Photoinduced magnetization of a cobalt-iron cyanide. *Science* **1996**, *272*, 704–705.
4. Amo-Ochoa, P.; Castillo, O.; Alexandre, S.S.; Welte, L.; de Pablo, P.J.; Rodriguez-Tapiador, I.; Gomez-Herrero, J.; Zamora, F. Synthesis of designed conductive one-dimensional coordination polymers of Ni(II) with 6-mercaptopurine and 6-thioguanine. *Inorg. Chem.* **2009**, *48*, 7931–7936.

5. Ichikawa, S.; Kimura, S.; Takahashi, K.; Mori, H.; Yoshida, G.; Manabe, Y.; Matsuda, M.; Tajima, H.; Yamaura, J.-I. Intrinsic carrier doping in antiferromagnetically interacted supramolecular copper complexes with (pyrazino)tetrathiafulvalene (pyra-TTF) as the ligand, $[Cu^{II}Cl_2(pyra\text{-}TTF)]$ and $(pyra\text{-}TTF)_2[Cu^{I}_3Cl_4(pyra\text{-}TTF)]$. *Inorg. Chem.* **2008**, *47*, 4140–4145.
6. Kishida, H.; Ito, T.; Nakamura, A.; Takaishi, S.; Yamashita, M. Current oscillation originating from negative differential resistance in one-dimensional halogen-bridged nickel compounds. *J. Appl. Phys.* **2009**, *106*, 016106:1–016106:3.
7. Mitsumi, M.; Murase, T.; Kishida, H.; Yoshinari, T.; Ozawa, Y.; Toriumi, K.; Sonoyama, T.; Kitagawa, H.; Mitani, T. Metallic behavior and periodical valence ordering in a MMX chain compound, $Pt_2(EtCS_2)_4I$. *J. Am. Chem. Soc.* **2001**, *123*, 11179–11192.
8. Miyasaka, H.; Motokawa, N.; Matsunaga, S.; Yamashita, M.; Sugimoto, K.; Mori, T.; Toyota, N.; Dunbar, K.R. Control of charge transfer in a series of Ru_2(II,II)/TCNQ two-dimensional networks by tuning the electron affinity of TCNQ units: A route to synergistic magnetic/conducting materials. *J. Am. Chem. Soc.* **2010**, *132*, 1532–1544.
9. Otsubo, K.; Kobayashi, A.; Kitagawa, H.; Hedo, M.; Uwatoko, Y.; Sagayama, H.; Wakabayashi, Y.; Sawa, H. Most stable metallic phase of the mixed-valence MMX-chain, $Pt_2(dtp)_4I$ (dtp = $C_2H_5CS_2^-$), in purely d-electronic conductors based on the transition-metal complex. *J. Am. Chem. Soc.* **2006**, *128*, 8140–8141.
10. Tadokoro, M.; Yasuzuka, S.; Nakamura, M.; Shinoda, T.; Tatenuma, T.; Mitsumi, M.; Ozawa, Y.; Toriumi, S.; Tatenuma, T.; Mitsumi, M.; Ozawa, Y.; Toriumi, K.; Yoshino, H.; Shiomi, D.; Sato, K.; Takui, T.; Mori, T.; Murata, K. A high-conductivity crystal containing a copper(I) coordination polymer bridged by the organic acceptor TANC. *Angew. Chem. Int. Ed.* **2006**, *45*, 5144–5147.
11. Zhong, J.C.; Misaki, Y.; Munakata, M.; Kuroda-Sowa, T.; Maekawa, M.; Suenaga, Y.; Konaka, H. Silver(I) coordination polymer of 2,5-Bis- (4',5'-bis(methylthio)-1',3'-dithiol-2'-ylidene)-1,3,4,6-tetrathiapentalene (TTM-TTP) and its highly conductive iodine derivative. *Inorg. Chem.* **2001**, *40*, 7096–7098.
12. Okubo, T.; Tanaka, N.; Kim, K.H.; Yone, H.; Maekawa, M.; Kuroda-Sowa, T. Magnetic and conducting properties of new halide-bridged mixed-valence CuI-CuII 1D coordination polymers including a hexamethylene dithiocarbamate ligand. *Inorg. Chem.* **2010**, *49*, 3700–3702.
13. Okubo, T.; Tanaka, N.; Kim, K.H.; Anma, H.; Seki, S.; Saeki, A.; Maekawa, M.; Kuroda-Sowa, T. Crystal structure and carrier transport properties of a new 3D mixed-valence Cu(I)-Cu(II) coordination polymer including pyrrolidine dithiocarbamate ligand. *Dalton Trans.* **2011**, *40*, 2218–2224.
14. Kim, K.H.; Ueta, T.; Okubo, T.; Hayami, S.; Anma, H.; Kato, K.; Shimizu, T.; Fujimori, J.; Maekawa, M.; Kuroda-Sowa, T. Synthesis and conducting properties of a new mixed-valence Cu(I)-Cu(II) 1-D coordination polymer bridged by morpholine dithiocarbamate. *Chem. Lett.* **2011**, *40*, 1184–1186.
15. Xie, Y.-M.; Liu, J.-H.; Wu, X.-Y.; Zhao, Z.-G.; Zhang, Q.-S.; Wang, F.; Chen, S.-C.; Lu, C.-Z. New ferroelectric and nonlinear optical porous coordination polymer constructed from a rare $(CuBr)_\infty$ castellated chain. *Cryst. Growth Des.* **2008**, *8*, 3914–3916.

16. Ye, Q.; Song, Y.-M.; Wang, G.-X.; Chen, K.; Fu, D.-W.; Chan, P.W.H.; Zhu, J.-S.; Huang, S.D.; Xiong, R.-G. Ferroelectric metal-organic framework with a high dielectric constant. *J. Am. Chem. Soc.* **2006**, *128*, 6554–6555.
17. Zhang, W.; Xiong, R.-G.; Huang, S.D. 3D framework containing Cu_4Br_4 cubane as connecting node with strong ferroelectricity. *J. Am. Chem. Soc.* **2008**, *130*, 10468–10469.
18. Kitagawa, S.; Kitaura, R.; Noro, S.-I. Functional porous coordination polymers. *Angew. Chem. Int. Ed. Engl.* **2004**, *43*, 2334–2375.
19. Noro, S.-I. Rational synthesis and characterization of porous Cu(II) coordination polymers. *Phys. Chem. Chem. Phys.* **2010**, *12*, 2519–2531.
20. Yaghi, O.M.; O'Keeffe, M.; Ockwig, N.W.; Chae, H.K.; Eddaoudi, M.; Kim, J. Reticular synthesis and the design of new materials. *Nature* **2003**, *423*, 705–714.
21. Cho, S.-H.; Ma, B.; Nguyen, S.T.; Hupp, J.T.; Albrecht-Schmitt, T.E. A metal-organic framework material that functions as an enantioselective catalyst for olefin epoxidation. *Chem. Commun.* **2006**, 2563–2565.
22. Farrusseng, D.; Aguado, S.; Pinel, C. Metal-organic frameworks: Opportunities for catalysis. *Angew. Chem. Int. Ed.* **2009**, *48*, 7502–7513.
23. Uemura, T.; Kitaura, R.; Ohta, Y.; Nagaoka, M.; Kitagawa, S. Nanochannel-promoted polymerization of substituted acetylenes in porous coordination polymers. *Angew. Chem. Int. Ed.* **2006**, *45*, 4112–4116.
24. Zou, R.-Q.; Sakurai, H.; Xu, Q. Preparation, adsorption properties, and catalytic activity of three-dimensional porous metal-organic frameworks composed of cubic building blocks and alkali-metal ions. *Angew. Chem. Int. Ed.* **2006**, *45*, 2542–2546.
25. Enoki, T.; Miyazaki, A. Magnetic TTF-based charge-transfer complexes. *Chem. Rev.* **2004**, *104*, 5449–5477.
26. Montes, V.A.; Zyryanov, G.V.; Danilov, E.; Agarwal, N.; Palacios, M.A.; Anzenbacher, P. Ultrafast energy transfer in oligofluorene-aluminum bis(8-hydroxyquinoline)acetylacetone coordination polymers. *J. Am. Chem. Soc.* **2009**, *131*, 1787–1795.
27. Kim, K.H.; Okubo, T.; Tanaka, N.; Mimura, N.; Maekawa, M.; Kuroda-Sowa, T. Dye-sensitized solar cells with halide-bridged mixed-valence Cu(I)-Cu(II) coordination polymers with hexamethylenedithiocarbamate ligand. *Chem. Lett.* **2010**, *39*, 792–793.
28. Tang, C.W. Two-layer organic photovoltaic cell. *Appl. Phys. Lett.* **1986**, *48*, 183–185.
29. Hiramoto, M.; Fujiwara, H.; Yokoyama, M. Three-layered organic solar cell with a photoactive interlayer of codeposited pigments. *Appl. Phys. Lett.* **1991**, *58*, 1062–1064.
30. O'Regan, B.; Graetzel, M. A low-cost, high-efficiency solar cell based on dye-sensitized colloidal titanium dioxide films. *Nature* **1991**, *353*, 737–740.
31. Graetzel, M. Solar energy conversion by dye-sensitized photovoltaic cells. *Inorg. Chem.* **2005**, *44*, 6841–6851.
32. Li, T.-L.; Lee, Y.-L.; Teng, H. $CuInS_2$ quantum dots coated with CdS as high-performance sensitizers for TiO_2 electrodes in photoelectrochemical cells. *J. Mater. Chem.* **2011**, *21*, 5089–5098.

33. Jian, F.; Wang, Z.; Bai, Z.; You, X.; Fun, H.-K.; Chinnakali, K.; Razak, I.A. The crystal structure, equilibrium and spectroscopic studies of bis(dialkyldithiocarbamate) copper(II) complexes $[Cu_2(R_2dtc)_4]$ (dtc = dithiocarbamate). *Polyhedron* **1999**, *18*, 3401–3406.
34. Ngo, S.C.; Banger, K.K.; DelaRosa, M.J.; Toscano, P.J.; Welch, J.T. Thermal and structural characterization of a series of homoleptic Cu(II) dialkyldithiocarbamate complexes: Bigger is only marginally better for potential MOCVD performance. *Polyhedron* **2003**, *22*, 1575–1583.
35. Sheldrick, G.M. A short history of SHELX. *Acta Crystallogr. A* **2008**, *A64*, 112–122.
36. Burla, M.C.; Caliandro, R.; Camalli, M.; Carrozzini, B.; Cascarano, G.L.; de Caro, L.; Giacovazzo, C.; Polidori, G.; Siliqi, D.; Spagna, R. IL MILIONE: A suite of computer programs for crystal structure solution of proteins. *J. Appl. Crystallogr.* **2007**, *40*, 609–613.
37. Least Squares function minimized (SHELX97): $\Sigma w(F_O^2-F_C^2)^2$ where w = Least Squares weights.
38. Crystal Structure Analysis Package, Rigaku Corporation (200-2010) Tokyo 196-8666, Japan.
39. Crystal data for $[Cu_2NiBr_2(Hm\text{-}dtc)_2(CH_3CN)_2]_n$: fw 776.30, monoclinic, $P2_1/c$, a = 10.3600(6) Å, b = 8.1909(5) Å, c = 15.962(2) Å, β = 105.983(3)°, V = 1302.1(2) Å^3, Z = 2, D_{calcd} = 1.980 g/cm^3, 12132 reflections measured, 2966 were unique. R_1 = 0.0315 ($I > 2.00\sigma(I)$), wR_2 = 0.0775 (all data). CCDC: 889235.
40. Ramalingam, K.; Radha, K.; Aravamudan, G.; Mahadevan, C.; Subramanyam, C.; Seshasayee, M. Structure of bis[*N,N*-bis(2-hydroxyethyl)dithiocarbamato]nickel(II), $C_{10}H_{20}N_2NiO_4S_4$. *Acta Crystallogr. C* **1984**, *C40*, 1838–1839.
41. Radha, A.; Seshasayee, M.; Aravamudan, G. Structures of bis(piperidine-1-dithiocarbamato)nickel(II) and bis(piperidine-1-dithiocarbamato)copper(II). *Acta Crystallogr. C* **1988**, *C44*, 1378–1381.
42. Srinivasan, S.; Ramalingam, K.; Rizzoli, C. Synthesis, NMR and single crystal X-ray structural studies on planar NiS_4 and NiS_2PN chromophores: Steric and electronic effects. *Polyhedron* **2012**, *33*, 60–66.
43. Hogarth, G.; Rainford-Brent, E.-J.C.-R.C.R.; Richards, I. Functionalised dithiocarbamate complexes: Synthesis and molecular structures of bis(2-methoxyethyl)dithiocarbamate complexes $[M\{S_2CN(CH_2CH_2OMe)_2\}_2]$ (M = Ni, Cu, Zn) and $[Cu\{S_2CN(CH_2CH_2OMe)_2\}_2][ClO_4]$. *Inorg. Chim. Acta* **2009**, *362*, 1361–1364.
44. Brese, N.E.; O'Keeffe, M. Bond-valence parameters for solids. *Acta Crystallogr. B* **1991**, *B47*, 192–197.
45. Crystal data for $[Cu_2NiI_2(Hm\text{-}dtc)_2(CH_3CN)_2]_n$: fw 870.30, monoclinic, $P2_1/c$, a = 10.3943(8) Å, b = 8.2724(6) Å, c = 16.385(2) Å, β = 106.045(3)°, V = 1354.0(2) Å^3, Z = 2, D_{calcd} = 2.135 g/cm^3, 12486 reflections measured, 3060 were unique. R_1 = 0.0262 ($I > 2.00\sigma(I)$), wR_2 = 0.0651 (all data). CCDC: 889238.
46. Ivanov, A.V.; Ivakhnenko, E.V.; Forsling, W.; Gerasimenko, A.V.; Bukvetskii, B.V. A comparative study of the structural organization of nickel(II) and copper(II) complexes with dialkyl-substituted and cyclic diethyldithiocarbamate ligands by X-ray crystallography, EPR, and CP/MAS 13C and 15N NMR. *Russ. J. Inorg. Chem.* **2002**, *47*, 410–422.
47. Kubelka, P. New contributions to the optics of intensely light-scattering materials. *J. Opt. Soc. Am.* **1948**, *38*, 448–457.

48. Nazeeruddin, M.K.; Kay, A.; Rodicio, I.; Humphry-Baker, R.; Mueller, E.; Liska, P.; Vlachopoulos, N.; Graetzel, M. Conversion of light to electricity by cis-X_2bis(2,2'-bipyridyl-4,4'-dicarboxylate)ruthenium(II) charge-transfer sensitizers (X = Cl^-, Br^-, I^-, CN^-, and SCN^-) on nanocrystalline TiO_2 electrodes *J. Am. Chem. Soc.* **1993**, *115*, 6382–6390.
49. Zhang, S.; Yanagida, M.; Yang, X.; Han, L. Effect of 4-tert-butylpyridine on the quasi-Fermi level of dye-sensitized TiO_2 films. *Appl. Phys. Express* **2011**, *4*, 042301:1–042301:3.